Staggered and short-period solutions of the saturable discrete nonlinear Schrödinger equation

2009 J. Phys. A: Math. Theor. 42 085002

(http://iopscience.iop.org/1751-8121/42/8/085002)

IOP PUBLISHING JOURNAL OF PHYSICS A: MATHEMATICAL AND THEORETICAL

J. Phys. A: Math. Theor. **42** (2009) 085002 (6pp) doi:10.1088/1751-8113/42/8/085002

Staggered and short-period solutions of the saturable discrete nonlinear Schrödinger equation

Avinash Khare[1], **Kim Ø Rasmussen**[2], **Mogens R Samuelsen**[3] **and Avadh Saxena**[2]

[1] Institute of Physics, Bhubaneswar, Orissa 751005, India
[2] Theoretical Division and Center for Nonlinear Studies, Los Alamos National Laboratory, Los Alamos, NM, 87545, USA
[3] Department of Physics, The Technical University of Denmark, DK-2800 Kgs. Lyngby, Denmark

Received 17 September 2008, in final form 2 December 2008
Published 22 January 2009
Online at stacks.iop.org/JPhysA/42/085002

Abstract

We point out that the nonlinear Schrödinger lattice with a saturable nonlinearity also admits staggered periodic as well as localized pulse-like solutions. Further, the same model also admits solutions with a short period. We examine the stability of these solutions and find that the staggered as well as the short-period solutions are stable in most cases. We also show that the effective Peierls–Nabarro barrier for the pulse-like soliton solutions is zero.

PACS numbers: 05.45.Ra, 63.20.Ry, 63.20.Pw

The saturable discrete nonlinear Schrödinger (DNLS) equation is increasingly finding applications in various physical situations. Most notably it serves as a model for optical pulse propagation in optically modulated photorefractive media [1], and in this context the pulse dynamics it describes have been intensely studied [2–4]. In addition to its important role for such applications the saturable DNLS equation is also of interest from a purely nonlinear science viewpoint [5–7]. This interest arises because the saturable DNLS equation has been demonstrated [8] to admit onsite and intersite soliton solutions, which have the same energy. This is in contrast to the standard cubic nonlinear Schrödinger lattice where the onsite solution always has lower energy than the intersite solution. This phenomenon has often been characterized in terms of a so-called Peierls–Nabarro (PN) barrier, which is the energy difference between these two distinct solutions. Thus the particular feature of the saturable DNLS equation is that it allows the PN barrier to change sign and specifically vanish for certain solutions. The vanishing of the PN barrier has been associated with the ability of these solutions to translate undisturbed through the lattice, which is impossible in the cubic DNLS equation. Here we derive analytical solutions to the saturable DNLS equation and demonstrate that the localized soliton solutions have a zero PN barrier.

Recently, we obtained [9] two different temporally and spatially periodic solutions to the saturable equation[4]

$$\mathrm{i}\dot{\psi}_n + (\psi_{n+1} + \psi_{n-1} - 2\psi_n) + \frac{\nu|\psi_n|^2}{1+\mu|\psi_n|^2}\psi_n = 0, \tag{1}$$

where ψ_n is a complex valued 'wavefunction' at site n, while ν and μ are real parameters. In particular, the first solution is

$$\psi_n^{\mathrm{I}} = \frac{1}{\sqrt{\mu}}\frac{\mathrm{sn}(\beta, m)}{\mathrm{cn}(\beta, m)}\,\mathrm{dn}([n+c]\beta, m)\exp(-\mathrm{i}[\omega t + \delta]), \tag{2}$$

where the modulus of the elliptic functions m must be chosen such that

$$2 - \omega = \frac{\nu}{\mu} = \frac{2\mathrm{dn}(\beta, m)}{\mathrm{cn}^2(\beta, m)}, \qquad \beta = \frac{2K(m)}{N_p}, \tag{3}$$

and c and δ are arbitrary constants. We only need to consider c between 0 and $\frac{1}{2}$ (half the lattice spacing). Here $K(m)$ denotes the complete elliptic integral of the first kind [10]. The second solution is

$$\psi_n^{\mathrm{II}} = \sqrt{\frac{m}{\mu}}\frac{\mathrm{sn}(\beta, m)}{\mathrm{dn}(\beta, m)}\,\mathrm{cn}([n+c]\beta, m)\exp(-\mathrm{i}[\omega t + \delta]), \tag{4}$$

where the modulus m is now determined such that

$$2 - \omega = \frac{\nu}{\mu} = \frac{2\mathrm{cn}(\beta, m)}{\mathrm{dn}^2(\beta, m)}, \qquad \beta = \frac{4K(m)}{N_p}. \tag{5}$$

The integer N_p denotes the spatial period of the solutions. In the limit $N_p \to \infty$ ($m \to 1$), both the solutions ψ_n^{I} and ψ_n^{II} reduce to the same localized solution

$$\psi_n^{\mathrm{III}} = \frac{1}{\sqrt{\mu}}\frac{\sinh(\beta)}{\cosh([n+c]\beta)}\,\mathrm{e}^{-\mathrm{i}[\omega t+\delta]}, \qquad (N_p \to \infty), \tag{6}$$

where β is now given by

$$2 - \omega = \frac{\nu}{\mu} = 2\cosh\beta. \tag{7}$$

In [9], we also developed the stability analysis and examined the linear stability of these solutions to show that the solutions are linearly stable in most cases.

The purpose of this paper is to point out that the same model (1) also admits the corresponding staggered solutions. In particular, using the identities for the Jacobi elliptic functions [11], it is easily shown that the model admits the following solutions:

$$\psi_n^{\mathrm{IS}} = (-1)^n\frac{1}{\sqrt{\mu}}\frac{\mathrm{sn}(\beta, m)}{\mathrm{cn}(\beta, m)}\,\mathrm{dn}([n+c]\beta, m)\exp(-\mathrm{i}[\omega t + \delta]), \tag{8}$$

where the modulus m must be chosen such that

$$\omega - 2 = -\frac{\nu}{\mu} = \frac{2\mathrm{dn}(\beta, m)}{\mathrm{cn}^2(\beta, m)}, \qquad \beta = \frac{2K(m)}{N_p}, \tag{9}$$

$$\psi_n^{\mathrm{IIS}} = (-1)^n\sqrt{\frac{m}{\mu}}\frac{\mathrm{sn}(\beta, m)}{\mathrm{dn}(\beta, m)}\,\mathrm{cn}([n+c]\beta, m)\exp(-\mathrm{i}[\omega t + \delta]), \tag{10}$$

[4] Note that rewriting $\frac{\nu|\psi_n|^2}{1+\mu|\psi_n|^2}\psi_n = \frac{\nu}{\mu}\left(1 - \frac{1}{1+\mu|\psi_n|^2}\right)\psi_n$ and the notation change $\frac{\nu}{\mu} \to -\nu$ followed by the gauge transformation $\phi_n \to \phi_n \exp(-\nu t)$ render the equation in a form that is used more often [7].

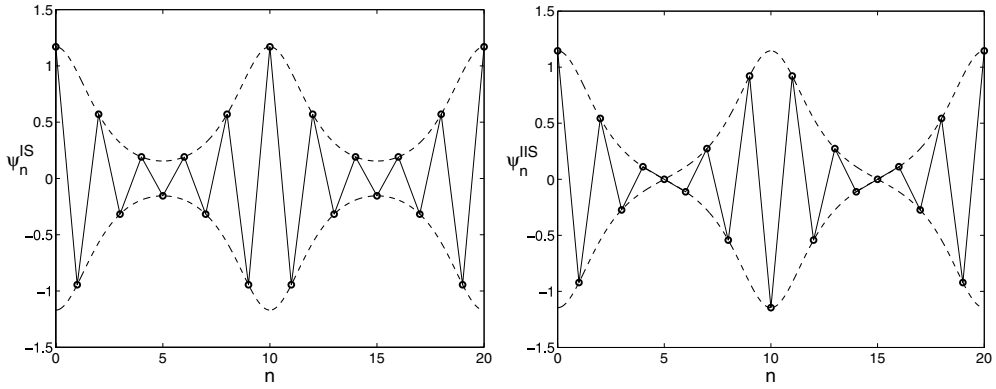

Figure 1. Illustration of the exact solutions of the two types. The parameters are: $\nu = -1$, $\mu = 0.4$, $\omega = 4.5$ and $c = t = \delta = 0$. $N_p = 10$ for ψ_n^{IS} and 20 for ψ_n^{IIS}. The dashed curves represent the solutions given by equations (8) and (10) as if n is a continuous variable. Lines are guides to the eye.

where the modulus m is now determined such that

$$\omega - 2 = -\frac{\nu}{\mu} = \frac{2\mathrm{cn}(\beta, m)}{\mathrm{dn}^2(\beta, m)}, \qquad \beta = \frac{4K(m)}{N_p}. \tag{11}$$

In the limit $N_p \to \infty$ ($m \to 1$), both the solutions ψ_n^{IS} and ψ_n^{IIS} reduce to the same localized staggered solution:

$$\psi_n^{\mathrm{IIIS}} = (-1)^n \frac{1}{\sqrt{\mu}} \frac{\sinh(\beta)}{\cosh([n+c]\beta)} \mathrm{e}^{-\mathrm{i}[\omega t + \delta]}, \qquad (N_p \to \infty), \tag{12}$$

where β is now given by

$$\omega - 2 = -\frac{\nu}{\mu} = 2\cosh\beta. \tag{13}$$

As an illustration we have plotted the exact solutions of the type IS and IIS in figure 1. Here the period N_p has to be even. We have shown two periods for type IS and only one for type IIS.

There are, as expressed by equations (9), (11) and (13), stringent conditions on the parameters μ and ν for which these exact solutions exist. For example, while the nonstaggered solutions are valid only for $\nu > 0$ and hence $\omega < 2$, the staggered solutions are valid only if $\nu < 0$ and hence $\omega > 2$. In the case IS, the limitation is

$$0\,(m = 1) < -\frac{2\mu}{\nu} < \cos^2\left(\frac{\pi}{N_p}\right) \quad (m = 0), \tag{14}$$

while in the case IIS the limitation is

$$0\,(m = 1) < -\frac{2\mu}{\nu} < \frac{1}{\cos\left(\frac{2\pi}{N_p}\right)} \quad (m = 0). \tag{15}$$

Similarly, the solution ψ_n^{IIIS} exists only when $-\frac{2\mu}{\nu}$ is close to zero ($m = 1$).

We have also examined the linear stability of these solutions and find that the solutions are linearly stable in most cases. A single period ($N = N_p$, where N is the lattice size) is always stable for both the solutions IS and IIS. A type IIS solution with more than one period

($N = jN_p$, where j is an integer larger than 1) is also stable, while a type IS solution with more than one period is always unstable. Thus, the first example in figure 1 is in fact unstable.

For the solution IIIS, expressions for both the power and Hamiltonian are identical to those for the solution III and are given by equations (13) and (14) of [9]. Hence the PN barrier for the solutions III and IIIS is the same. We would like to point out here that the calculation of PN barrier in I was not quite correct. In particular, since both power P and the Hamiltonian H are constants of motion, one must compute the energy difference between the solutions when $c = 0$ and $c = 1/2$ in such a way that the power P is *same* in both the cases. On using the expressions for P and H as given by equations (13) and (14) of [9], we find that H for the solution III as well as IIIS is given by

$$H = -\frac{4\sinh(\beta)}{\mu} + \frac{2\beta\nu}{\mu^2} + 2\left(1 - \frac{\nu}{2\mu}\right) P. \tag{16}$$

Note that H is in fact independent of c, i.e. in contrast to our claim in [9], the PN barrier is in fact zero for our solution III (and hence also for IIIS).

Before completing this paper, we would like to mention that the model (1) also admits a few short-period solutions.

Using the ansatz,

$$\psi_n(t) = \phi_n \, \mathrm{e}^{-\mathrm{i}(\omega t + \delta)}, \tag{17}$$

in equation (1), it is easily checked that the only possible short-period solutions to equation (1) are:

(i) Period 1 solution $\phi_n = (\ldots, a, a, \ldots)$ provided

$$\omega = -\frac{\nu a^2}{1 + \mu a^2}. \tag{18}$$

(ii) Period 2 solution $\phi_n = (\ldots, a, -a, \ldots)$ provided

$$\omega = 4 - \frac{\nu a^2}{1 + \mu a^2}. \tag{19}$$

(iii) Period 3 solution $\phi_n = (\ldots, a, 0, -a, \ldots)$ provided

$$\omega = 3 - \frac{\nu a^2}{1 + \mu a^2}. \tag{20}$$

(iv) Period 4 solutions $\phi_n = (\ldots, a, 0, -a, 0, \ldots)$ and $(\ldots, a, a, -a, -a, \ldots)$ provided

$$\omega = 2 - \frac{\nu a^2}{1 + \mu a^2}. \tag{21}$$

(v) Period 6 solution $\phi_n = (\ldots, a, a, 0, -a, -a, 0, \ldots)$ provided

$$\omega = 1 - \frac{\nu a^2}{1 + \mu a^2}. \tag{22}$$

Applying the stability analysis developed in [9] we have examined the stability of these short-period solutions and find that for a small nonlinearity ($|\nu| < 2\mu$) they are all stable. The period 4 solution $(\ldots, a, a, -a, -a, \ldots)$ is always stable while all the other short-period solutions possess regions of instabilities at larger nonlinearity. For these low-period solutions the stability matrices given by equations (20) and (21) of [9] are simple, and it is, for example, easy to see that the lowest non-zero eigenvalue, $\lambda_1(a, \nu)$, of the stability problem for the period 1 solutions is given by ($\mu = 1$)

$$\lambda_1(a, \nu) = a^4 + \left(2 - \tfrac{2}{3}\nu\right) a^2 + 1. \tag{23}$$

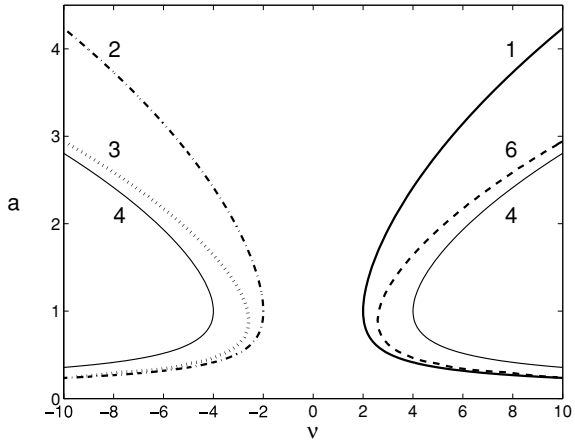

Figure 2. Regions of stability for the short-period solutions to equation (1) for $\mu = 1$. Period 1: thick full curve, period 2: dashed-dotted curve, period 3: long-dashed curve, period 4: thin full curve and period 6: long-dashed curve. The instability occurs in the parameter region encompassed by the respective curves.

Similarly, we have for the period 2 solution

$$\lambda_2(a, \nu) = a^4 + \left(2 + \tfrac{2}{3}\nu\right) a^2 + 1, \tag{24}$$

and for the period 4 solution

$$\lambda_4(a, \nu) = a^4 + (2 - |\nu|)a^2 + 1. \tag{25}$$

It is possible to derive similar expressions for the period 3 and period 6 solutions but the expressions are more complicated and will be omitted here. Clearly, the p period solutions are unstable for the parameter values where $\lambda_p(a, \nu) < 0$, and we have illustrated these regions in figure 2. Figure 2 shows the curves in the (a, ν)-plane where $\lambda_p(a, \nu) = 0$ so that the instability occurs in the regions that are encompassed by the respective curves. A symmetry is apparent in this stability diagram, and it is easy to realize that this symmetry arises from the fact that the transformation $(\nu, \phi_n) \rightarrow (-\nu, (-1)^n \phi_n)$ establishes the following connection between the short-period solutions: $1 \leftrightarrow 2$, $3 \leftrightarrow 6$ and $4 \leftrightarrow 4$.

In conclusion, we have obtained staggered as well as short-period solutions of the saturable discrete nonlinear Schrödinger equation. We also studied the linear stability and found the solutions to be stable in certain parameter ranges. Finally, we found that the Peierls–Nabarro barrier for the pulse solutions is zero. Our results are relevant to optical soliton pulse propagation in waveguides and photorefractive media [1].

Acknowledgments

Research at Los Alamos National Laboratory is carried out under the auspices of the National Nuclear Security Administration of the US Department of Energy under contract no DE-AC52-06NA25396.

References

[1] Fleischer J W 2005 *Opt. Express* **13** 1780
[2] Fitrakis E P, Kevrekidis P G, Malomed B A and Frantzeskakis D J 2006 *Phys. Rev.* E **74** 026605

[3] Vicencio R A and Johansson M 2006 *Phys. Rev.* E **73** 046602
[4] Cuevas J and Eilbeck J C 2006 *Phys. Lett.* A **358** 15
[5] Melvin T R O, Champneys A R and Kevrekidis P G 2006 *Phys. Rev. Lett.* **97** 124101
[6] Oxtoby O F and Barashenkov I V 2007 *Phys. Rev.* E **76** 036603
[7] Melvin T R O, Champneys A R and Kevrekidis P G 2008 *Physica* D **237** 551
[8] Hadzievskii L, Maluckov A, Stepic M and Kip D 2004 *Phys. Rev. Lett.* **93** 033901
[9] Khare A, Rasmussen K Ø, Samuelsen M R and Saxena A 2005 *J. Phys. A: Math. Gen.* **38** 807
[10] Abramowitz M and Stegun I A (ed) 1964 *Handbook of Mathematical Functions with Formulas, Graphs, and Mathematical Tables* (Washington, DC: US GPO)
[11] Khare A and Sukhatme U 2002 *J. Math. Phys.* **43** 3798
Khare A, Lakshminarayan A and Sukhatme U 2003 *J. Math. Phys.* **44** 1822 (arXiv:math-ph/0306028)
Khare A, Lakshminarayan A and Sukhatme U 2004 *Pramana J. Phys.* **62** 1201